1-1-2013

A novel method of embedding additional information into tensor diffusion filtering as an application for multi-modal reconstruction in ET

D Kazantsev
Malet Place Engineering

Sebastien Ourselin
University College London

Brian F. Hutton
University of Wollongong

W. R B. Lionheart
University of Manchester

Simon Arridge
University College London

A novel method of embedding additional information into tensor diffusion filtering as an application for multi-modal reconstruction in ET

Abstract

The fast development of hybrid imaging modalities in tomography, such as SPECT (single photon emission computed tomography)/CT (computed tomography), PET (positron emission tomography)/MRI (magnetic resonance imaging) and PET/CT, have increased an interest for reconstruction algorithms which are able to utilize a functional and anatomical information at the same time. In this paper a new method proposed for iterative reconstruction with anatomical prior in emission tomography (ET). The introduced regularization term is a modified anisotropic tensor diffusion filter which has shape-adapted smoothing properties. The filter accommodates available anatomical information which results in enhanced position and image dependent spatial resolution of emission images. Based on underlying orientations of normal and tangential vector fields for emission and anatomical images, the diffusion flux is rotated and scaled. Poisson likelihood fidelity and penalty terms are optimized separately by means of forward-backward splitting (FBS) technique. Presented approach is validated quantitatively using co-registered SPECT/MR synthetic data and compared with another anatomically penalized reconstruction as well as with iterative statistical reconstruction without regularization.

Keywords

method, additional, information, into, tensor, diffusion, filtering, application, multi, modal, reconstruction, et, novel, embedding

Disciplines

Engineering | Science and Technology Studies

Publication Details

Kazantsev, D., Ourselin, S., Hutton, B. F., Lionheart, W. R. B. & Arridge, S. R. (2013). A novel method of embedding additional information into tensor diffusion filtering as an application for multi-modal reconstruction in ET. Fully Three-Dimensional Image Reconstruction in Radiology and Nuclear Medicine Proceedings (pp. 312-315). United States: Fully 3D.

A novel method of embedding additional information into tensor diffusion filtering as an application for multi-modal reconstruction in ET

D. Kazantsev[1], S. Ourselin[2], B. F. Hutton[3], W.R.B. Lionheart[4] and S. R. Arridge[2]

***Abstract*—The fast development of hybrid imaging modalities in tomography, such as SPECT (single photon emission computed tomography)/CT (computed tomography), PET (positron emission tomography)/MRI (magnetic resonance imaging) and PET/CT, have increased an interest for reconstruction algorithms which are able to utilize a functional and anatomical information at the same time.**

In this paper a new method proposed for iterative reconstruction with anatomical prior in emission tomography (ET). The introduced regularization term is a modified anisotropic tensor diffusion filter which has shape-adapted smoothing properties. The filter accommodates available anatomical information which results in enhanced position and image dependent spatial resolution of emission images. Based on underlying orientations of normal and tangential vector fields for emission and anatomical images, the diffusion flux is rotated and scaled. Poisson likelihood fidelity and penalty terms are optimized separately by means of forward-backward splitting (FBS) technique. Presented approach is validated quantitatively using co-registered SPECT/MR synthetic data and compared with another anatomically penalized reconstruction as well as with iterative statistical reconstruction without regularization.

***Index Terms*—emission tomography, hybrid modalities, anatomical prior, image denoising, tensor diffusion, anisotropy, regularization, splitting methods**

I. Introduction

For reconstruction of activity distribution in ET, iterative statistical methods, such as, maximum-likelihood expectation maximization (MLEM) algorithm [1] are commonly used. Since the reconstruction problem in ET is ill-posed and ill-conditioned it requires additional regularization to ensure well-posedness. From a Bayesian perspective, imposing desirable properties (e.g. smoothness) on the solution leads to a prior probability characterization. A maximum *a posteriori* probability (MAP) estimate or penalized likelihood are successful methods employing the prior information. In the tomographic reconstruction, the sum of the likelihood penalized by the noise suppressing term is optimized [2].

The use of variational regularization techniques for tomographic reconstruction is significantly supported by the successful development of image processing tools and corresponding mathematical framework [3]. Successfully dealing with noise in images while leaving important features intact, the penalties based on partial differential equations (PDE), such as total variation (TV) [4] and anisotropic diffusion (AD) [5],[6] are competitive means to regularize reconstruction in emission tomography (ET).

The availability of side information from hybrid scanners (SPECT/CT, PET/MRI and PET/CT) can improve resolution of functional image by referring to prominent edges of anatomical data [7]. In this paper we propose a new method to smooth radiopharmaceutical distribution by means of available anatomical information. Although the proposed method has some similarities with previous work on modified diffusion filters [8], [9] it is based on a very new idea of embedding available data into the filtering process.

To reach a desired solution we utilize the FBS approach [10] for cost function iterative optimization. Cost function is decomposed into two sub-problems which are optimized separately. Similarly to [11] we split Poisson data fidelity and variational penalty terms. The resulting algorithm consists of the classical MLEM step followed by the modified diffusion step. The nature of the diffusion step is the main contribution of this paper.

II. Method

A. Tensor based anisotropic diffusion filtering (TBADF)

Following the Weickert's approach [5] for evaluation of local orientations of the image gradient $\nabla u(\mathbf{x})$ the *structure tensor* has to be build. Here we consider the 2D case ($\mathbf{x} = (x, y)$), however the proposed method can be easily generalized for the 3D. To avoid false edge detections due to noise, $u(\mathbf{x})$ is convolved with a Gaussian kernel k_σ, where σ is a *differentiation scale*: $u_\sigma(\mathbf{x}) = (k_\sigma * u)(\mathbf{x})$. The local information is averaged by convolving component-wise $\nabla u_\sigma \nabla u_\sigma^T$ with a Gaussian kernel k_ρ, where ρ is an *integration* scale which controls the size of the neighbourhood with gradients dominant orientations [3].

The structure tensor can be constructed as a symmetric, positive semidefinite (PSD) matrix:

$$\mathbf{J}_\rho(\nabla u_\sigma)(\mathbf{x}) = k_\rho * (\nabla u_\sigma \nabla u_\sigma^T). \tag{1}$$

Principal axis transformation of (1) gives the orthonormal eigenvectors $\boldsymbol{v_1} \parallel \nabla u_\sigma, \boldsymbol{v_2} \perp \nabla u_\sigma$, such as

$$\lim_{\rho \to 0} \boldsymbol{v_1} = \frac{\nabla u_\sigma}{|\nabla u_\sigma|} \;\; ; \;\; \lim_{\rho \to 0} \boldsymbol{v_2} = \frac{\nabla u_\sigma^\perp}{|\nabla u_\sigma|} \tag{2}$$

This work has been supported by the Engineering and Physical Sciences Research Council under grants EP/J010456/1, EP/I02249X/1 and EP/G026483/1. This research project has been supported by the European Commission under the 7th Framework Programme through the "Research Infrastructures" action of the "Capacities" Programme, NMI3-II Grant No. 283883, Project No.20120553

[1] The Manchester X-Ray Imaging Facility, School of Materials, The University of Manchester, Manchester, M13 9PL, UK (E-mail: daniil.kazantsev@manchester.ac.uk)

[2] Centre for Medical Image Computing, University College London, London NW1 9EE, UK

[3] Institute of Nuclear Medicine, UCL and University College London Hospitals NHS Trust, 235 Euston Road (T-5), London NW1 2BU, UK.

[4] School of Mathematics, Alan Turing Building, The University of Manchester, M13 9PL, UK

where $|\nabla u| = \sqrt{u_x^2 + u_y^2}$ and the corresponding eigenvalues defined using the PSD matrix components as:

$$\eta_{1,2} = \frac{1}{2}\left(j_{11} + j_{22} \pm \sqrt{(j_{11} - j_{22})^2 + 4j_{12}^2}\right), \tag{3}$$

The eigenvalues $\eta_{1,2}$ (averaged by the scale parameter ρ) convey the level of intensity propagation along the given directions $\boldsymbol{v_{1,2}}$. The eigenvalues characterize local geometrical information, for isotropic areas $\eta_1 \cong \eta_2 \cong 0$ and $\eta_1 \gg \eta_2$ or $\eta_1 \ll \eta_2$ for anisotropic (line structures).

Furthermore, based on $\eta_{1,2}$ one can estimate the level of anisotropy using the normalized measure of coherence [12]:

$$C(\mathbf{x}) = \left(\frac{\eta_1 - \eta_2}{\eta_1 + \eta_2}\right)^2; \quad C(\mathbf{x}) \in [0, 1], \tag{4}$$

when $C(\mathbf{x}) = 1$ the gradient is totally aligned, when $C(\mathbf{x}) = 0$ it has no preferred direction. Note that the measure (4) is undefined for the uniform regions.

The diffusion PDE in its general form can be written as:

$$\begin{cases} \partial_t u = \nabla \cdot (\mathbf{D}(\mathbf{J}_\rho(\nabla u_\sigma))\nabla u), \\ \qquad\qquad u(\mathbf{x}, 0) = u_0. \end{cases} \tag{5}$$

For $\mathbf{D} = \mathbf{I}$, (5) performs a linear isotropic diffusion, for $\mathbf{D} = \varphi(|\nabla u|)\mathbf{I}$ it is equivalent to a nonlinear isotropic diffusion (φ is an edge preserving function [5]), and for

$$\mathbf{D} = [\boldsymbol{v_1}\ \boldsymbol{v_2}] \cdot \begin{bmatrix} \gamma_1 & 0 \\ 0 & \gamma_2 \end{bmatrix} \cdot \begin{bmatrix} \boldsymbol{v_1}^T \\ \boldsymbol{v_2}^T \end{bmatrix} = \begin{bmatrix} D_{11} & D_{12} \\ D_{12} & D_{22} \end{bmatrix}, \tag{6}$$

equation (5) stands for anisotropic nonlinear diffusion driven by the diffusion tensor with elements:

$$D_{i,j} = \sum_{n=1,\dots,2} \gamma_n v_{ni} v_{nj}, \tag{7}$$

The diffusion tensor (6) has a new eigenvalues $\gamma_{1,2}$ which define the strength of smoothing in the preferred directions $\boldsymbol{v_{1,2}}$. A few different definitions for γ_n related to the edge enhancing diffusion (EED) and the coherence enhancing diffusion (CED) were proposed by Weickert [13]. In this paper we will be using the EED approach, where smoothing in normal direction is reduced by:

$$\gamma_1 = \varphi(|\nabla u|) = \exp\left(-|\nabla u|^2/\epsilon^2\right), \tag{8}$$

while the eigenvalue related to the tangential vector is $\gamma_2 = 1$. The threshold parameter ϵ controls the strength of diffusion. The diffusion tensor rotates and scales the flux in order to adapt it for underlying geometrical configurations of image $u(\mathrm{x})$.

B. *Embedding additional information into the TBADF*

Here we present a novel idea how to embed an additional information $\boldsymbol{\mu}$ into the image $\boldsymbol{\lambda}$ by means of the tensor based diffusion filtering.

Let us assume that the diffusion tensors $\mathbf{D}_\mu$ and $\mathbf{D}_\lambda$ are defined for images $\boldsymbol{\mu}$ and $\boldsymbol{\lambda}$ respectively.

The *combined* diffusion tensor can be defined using following arithmetic interpolation scheme between two given tensors [14] as:

$$\mathbf{D}_{\mu,\lambda} = s\mathbf{D}_\lambda + (1 - s)\mathbf{D}_\mu; \quad s(\mathbf{x}) \in [0, 1], \tag{9}$$

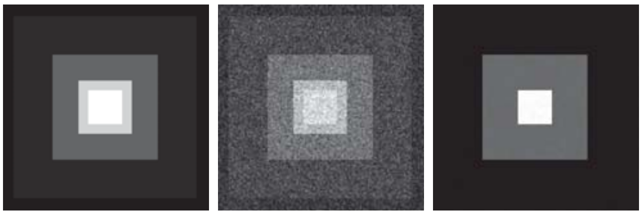

Fig. 1: From left to right: Original image, noisy image $\boldsymbol{\lambda}$ containing 10% of random noise and reference image $\boldsymbol{\mu}$ containing 1% of random noise.

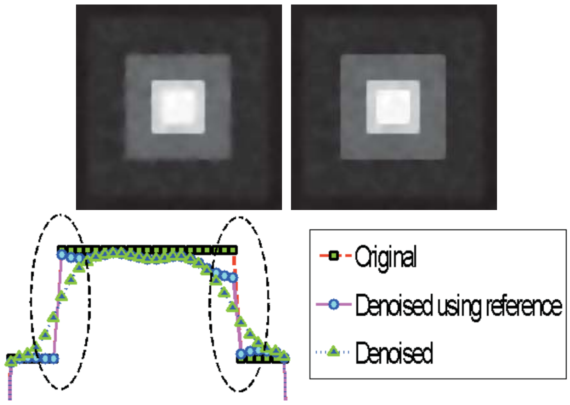

Fig. 2: Example of the TBAD filtering with a help of additional information. Top row from left to right: denoised image $\boldsymbol{\lambda}$ without use of the referenced image $\boldsymbol{\mu}$; filtered $\boldsymbol{\lambda}$ using the referenced image $\boldsymbol{\mu}$ and the combined tensor (9). Bottom picture is a plot of the horizontal middle section (the central region) of the denoised images above and the original image. In the marked areas edges are better preserved for the proposed method.

where $s(\mathrm{x})$ is a spatially variant parameter which should fulfil the following properties:

Property (1): $\forall \mathbf{x}$ calculate $\theta(\mathbf{x}) = acos(\boldsymbol{v_1}(\boldsymbol{\mu}) \cdot \boldsymbol{v_1}(\boldsymbol{\lambda}))$; if $\theta(\mathbf{x}) \in [0°, 0° + \theta_a]$ or $\theta \in [180° - \theta_a, 180°]$, then $s(\mathbf{x}) = 0$.

Property (2): $\forall s(\mathbf{x}) \neq 0$: $s(\mathbf{x}) = C_\lambda(\mathbf{x})$ (4).

Property (3): $\forall \mathbf{x}$ where $C_\lambda(\mathbf{x})$ is undefined: $s(\mathbf{x}) = 0$.

The ideas behind properties (1-3) are the following:

Property (1) is fulfilled when $C_\lambda(\mathbf{x}) \cong C_\mu(\mathbf{x}) \gg 0$, which is the case of an expressed anisotropy for both images. By checking angles between the two principal vector bases for images $\boldsymbol{\lambda}$ and $\boldsymbol{\mu}$ one can estimate how bases are agreed with each other. An *acceptance angle* θ_a is introduced as a threshold parameter to make a decision on overlapping degree of two vectors. Empirically we found that $\theta_a = 10°$ gives satisfying results. When property (1) is fulfilled for some $\mathbf{x}$, so $s(\mathbf{x}) = 0$, it gives $\mathbf{D}_{\mu,\lambda} = \mathbf{D}_\mu$, then the diffusion (5) is performed using diffusion tensor of image $\boldsymbol{\mu}$.

Property (2) ensures that all values of $s(\mathbf{x})$ which are not equal to zero should be equal to $C_\lambda(\mathbf{x})$. Based on the level of anisotropy of image $\boldsymbol{\lambda}$ the interpolation between two tensors (9) takes place. For areas with higher anisotropy on $\boldsymbol{\lambda}$ there is less influence of $\boldsymbol{\mu}$.

Property (3) considers the uniform regions of image $\boldsymbol{\lambda}$ where C_λ is undefined ($\eta_1(\lambda) + \eta_2(\lambda) = 0$). If C_μ is undefined as well, then $\mathbf{D} = \mathbf{I}$.

The proposed method was tested for the simple denoising

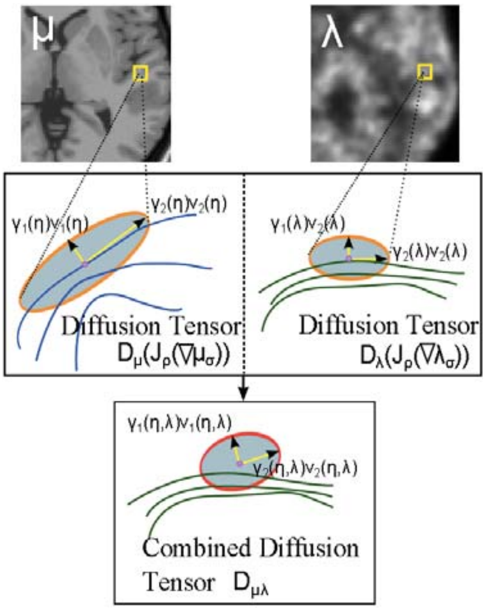

Fig. 3: The example of local geometrical structure represented by two diffusion tensors for anatomical $\boldsymbol{\mu}$ and emission images $\boldsymbol{\lambda}$. The combined diffusion tensor is constructed by interpolation (9).

procedure of image $\boldsymbol{\lambda}$ having additional image $\boldsymbol{\mu}$ as a reference, see Fig. 1. In Fig. 2 the results of the filtered image $\boldsymbol{\lambda}$ without use of referenced image $\boldsymbol{\mu}$ and with it. Note that for places where edges of exact image matched the reference sharp features are preserved, see plot in Fig. 2. This is the case when the property (1) is taken place. For areas where there is no additional information from $\boldsymbol{\mu}$ the property (2) performs.

The idea of the combined tensor filtering (9) can be used for the hybrid imaging modalities having emission data registered with anatomical one. The Fig. 3 explains how the combined tensor can be used for the problem of reconstruction in ET having data from MR scanner.

C. An anatomically driven tensor based anisotropic diffusion filtering (ADTBADF) for ET reconstruction

Lets consider the discrete activity distribution as N-dim vector $\boldsymbol{\lambda}$ with elements $\lambda_i, i = 1, \ldots, \mathrm{N}$ and $\boldsymbol{g}$ is a measured projection data (sinogram) with elements $g_j, j = 1, \ldots, \mathrm{M}$. In the ET, $\boldsymbol{g}$ follows Poisson distribution with mean $\overline{\boldsymbol{g}} = \mathrm{P}\boldsymbol{\lambda}$, where projection or system matrix $\mathrm{P} : \mathbb{R}^N \rightarrow \mathbb{R}^M$ depends on system design and detector array geometry.

To reconstruct desired image $\boldsymbol{\lambda}$ from Poisson distributed data $\boldsymbol{g}$, the following constrained cost function needs to be optimized:

$$\min_{\boldsymbol{\lambda}} \left\{ \mathbb{D}_{KL}(\boldsymbol{g}, \mathrm{P}\boldsymbol{\lambda}) + \beta \int_\Omega h(|\nabla \boldsymbol{\lambda}|) \mathrm{d}\Omega \right\} \quad \text{S.T. } \boldsymbol{\lambda} \geq 0, \quad (10)$$

where $\mathbb{D}_{KL}(\boldsymbol{g}, \mathrm{P}\boldsymbol{\lambda}) = \int [\overline{\boldsymbol{g}} - \boldsymbol{g} \log \overline{\boldsymbol{g}}]$ is a Kullback - Leibler distance and second term is a convex energy functional controlled by regularization parameter β [15].

The algorithms based on proximity operator properties [10] can solve (10) by splitting regularization and data-fidelity terms in a way that two (generally less complex) sub-problems have to be solved.

Similarly to [11], [8] a nested two step iteration algorithm can be derived in a form:

$$\begin{array}{rcll} \boldsymbol{\lambda}^{m+\frac{1}{2}} & = & \frac{\boldsymbol{\lambda}^m}{\mathrm{P}^*\mathbf{1}} \mathrm{P}^* \left(\frac{\boldsymbol{g}}{\mathrm{P}\boldsymbol{\lambda}^m} \right), & \textit{MLEM step} \\ \boldsymbol{\lambda}^{m+1} & = & \mathrm{L} \left(\boldsymbol{\lambda}^{m+\frac{1}{2}} \right) & \textit{Filtering step} \end{array} \quad (11)$$

Where L is a diffusion operator which performs transition from $\boldsymbol{\lambda}^{m+\frac{1}{2}}$ to $\boldsymbol{\lambda}^{m+1}$ by minimizing the following function:

$$\Psi(\boldsymbol{\lambda}) = \frac{1}{2} \int_\Omega \frac{\mathrm{P}^*\mathbf{1}}{\boldsymbol{\lambda}^m} \left(\boldsymbol{\lambda} - \boldsymbol{\lambda}^{m+\frac{1}{2}} \right)^2 + \beta \int_\Omega h(|\nabla \boldsymbol{\lambda}|) \mathrm{d}\Omega \quad (12)$$

In this work we use a standard iterative gradient descent algorithm to optimize (12):

$$\begin{cases} \boldsymbol{\lambda}^{l+1} = \boldsymbol{\lambda}^l + \tau(\Psi'(\boldsymbol{\lambda})) \\ \boldsymbol{\lambda}^1 = \boldsymbol{\lambda}^{m+\frac{1}{2}}, \end{cases} \quad (13)$$

$$\Psi'(\boldsymbol{\lambda}) = \frac{\mathrm{P}^*\mathbf{1}}{\boldsymbol{\lambda}^m} \left(\boldsymbol{\lambda} - \boldsymbol{\lambda}^{m+\frac{1}{2}} \right) + \beta(\nabla \cdot (\mathbf{D}_{\mu,\lambda} \nabla \boldsymbol{\lambda})). \quad (14)$$

The right part of (14) includes the sum of weighted data fidelity term and a nonlinear anisotropic diffusion term which includes the proposed combined tensor (9).

III. Numerical results

In this work we compare several reconstruction techniques, namely: an anatomically driven tensor based anisotropic diffusion filtering (ADTBADF) (11) with a filtering step (14), an anatomically driven nonlinear isotropic diffusion filtering (ADNIDF) with quadratic function (QADNIDF), with Huber function (HADNIDF) and classical MLEM (step 1 in (11)). The ADNIDF method is an iterative application of a Bowsher prior (a local activity smoothing technique based on intensity distribution in the neighbourhood of anatomical image, more in [16]) in the second step of (11). More information about this method can be found in [8].

For our experiments we used 2D synthetic Brainweb data to perform quantitative analysis of methods. The proposed algorithm can be generalized for 3D data, however the quantitative validation is much more time consuming in this case. The synthetic activity phantom is projected to form noise-free sinogram, then 30 Poisson noise realizations were generated from the data. Due to lack of space we are not presenting all necessary graphs for bias-variance analysis but we will comment on them.

In Fig. 4 one can see that the MLEM image has poor resolution and the highest variance for the hot lesion region of interest (ROI). However, the level of intensity in lesion ROI is high and the bias is very low. The use of quadratic smoothing with QADNIDF gives a significant enhancement of resolution of emission image (the smallest variance). The bias of QADNIDF is the highest due to over-smoothing of activity. The use of Huber function in HADNIDF can increase bias but as well as the variance. The reconstructed image with HADNIDF is less smooth (piecewise-constant appearance due to penalty function), but lesion is better quantified than with QADNIDF. The proposed approach (ADTBADF) allows to reduce bias further for approximately the same level of

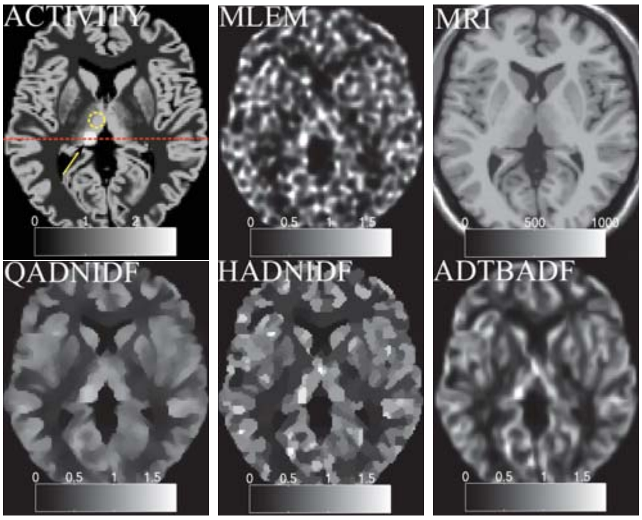

Fig. 4: left to right, top row: the 2D modeled activity phantom with hot lesion pointed by the arrow (the dotted circle was taken as a background region to calculate contrast for the lesion nearby and the background variance, MLEM reconstruction ($m = 170$) co-registered MR image; bottom row: reconstruction with QADNIDF, HADNIDF and ADTBADF.

variance. The value of variance is lowest for the gray matter region but the bias is slightly higher than for ADNIDF (edges are blurred due to convolution).

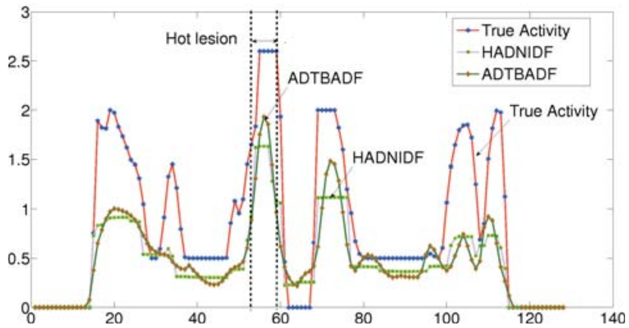

Fig. 5: 1D slices of the the true activity (horizontal line across the phantom in the Fig. 4), HADNIDF and ADTBADF images.

In the Fig. 5 one can see 1D slices of reconstructed images comparatively to original phantom. The proposed method gives smoother reconstruction but preserves an important features in data.

IV. DISCUSSION

The proposed algorithm has four additional parameters to control reconstruction comparatively to ADNIDF method (two Gaussian kernels σ, ρ in (1), the edge preserving threshold ϵ (8) for image μ and the angle of acceptance θ_a. However it doesn't add any significant difficulties to choose these parameters, first three can be estimated automatically based on the level of noise in image μ. The optimal threshold parameter ϵ is usually harder to determine in blurred images, a few suggestions for selection exist in literature [5]. In this work we didn't concentrate on this issue and the choice was empirical.

Here we present a binary decision procedure for the property (1) based on θ_a threshold. However due to noise and blur the local estimation of angles can be erroneous. Considering principal directions in a non-local region can improve property (1).

In ET reconstructed images are generally blurred (premature stop of the MLEM algorithm or smoothing penalty applied). The smooth appearance of the reconstructed images with the proposed method can be beneficial for clinicians who get used to visual assessment of similar images. The strength of blur for reconstructed images is controlled by width of Gaussian kernels and can be optimized.

V. CONCLUSION

In this work we present a novel approach of incorporating available additional information into diffusion filtering. The process of embedding information is performed by scaling and rotating the combined diffusion tensor of two images. Special properties of the proposed tensor were tested on the simple denoising example. The method shows the ability to detect matching directions of tensor fields of two images, it helps to retain edges and resolution in a filtered image.

The proposed method is tested for the modelled case of the SPECT reconstruction with co-registered MR data as a reference image. It produces better results in terms of bias, contrast and variance for lesions. Reconstructed images look more favourable due to smooth appearance and well preserved important features such as lesions.

REFERENCES

[1] A J Rockmore and A Macovski, “A maximum likelihood approach to emission image reconstruction from projections,” *IEEE Trans. Nucl. Sci.*, vol. 23, pp. 1428–1432, 1976.
[2] Alvaro R De Pierro, “A modified expectation maximization algorithm for penalized likelihood estimation in emission tomography,” *IEEE Trans. Med. Imag.*, vol. 14, pp. 132–137, 1995.
[3] G Aubert and P Kornprobst, “Mathematical problems in image processing. partial differential equations and the calculus of variations,” *Applied Mathematical Sciences.Springer.New York*, vol. 147, 2001.
[4] L I Rudin, S Osher, and E Fatemi, “Nonlinear total variation based noise removal algorithms,” *Physica D.*, vol. 60, pp. 259–268, 1992.
[5] J Weickert, “Anisotropic diffusion in image processing,” *Stuttgart, Germany: Teubner*, 1998.
[6] P Perona and J Malik, “Scale-space and edge detection using anisotropic diffusion,” *IEEE Trans. Pattern Analysis*, vol. 12, pp. 629–639, 1990.
[7] K Erlandsson, I Buvat, P H Pretorius, B A Thomas, and Hutton B F, “A review of partial volume correction techniques for emission tomography and their applications in neurology, cardiology and oncology,” *Physics in Medicine and Biology*, vol. 57, no. 21, pp. R119, 2012.
[8] D Kazantsev, S R Arridge, S Pedemonte, A Bousse, K Erlandsson, B F Hutton, and S Ourselin, “An anatomically driven anisotropic diffusion filtering method for 3d spect reconstruction,” *Phys Med. Biol.*, vol. 57, pp. 3793–3810, 2012.
[9] C Chan, R R Fulton, D D Feng, and S R Meikle, “Regularized image reconstruction with an anatomically adaptive prior for positron emission tomography,” *Phys Med. Biol.*, vol. 54, no. 24, pp. 7379–7400, 2009.
[10] P L Combettes and J C Pesquet, “Proximal splitting methods in signal processing,” *Fixed-Point Algorithms for Inverse Problems in Science and Engineering, Eds. New York: Springer-Verlag*, vol. 10, 2010.
[11] A Sawatzky, C Brune, F Wubbeling, T Kosters, K Schafers, and M Burger, “Accurate em-tv algorithm in pet with low snr,” in *IEEE Nucl. Sci. Symp. Conf. Rec.*, 2008, pp. 5133–5137.
[12] B Jahne, “Spatio-temporal image processing: Theory and scientific applications,” *Berlin: Springer-Verlag*, vol. 751, no. 0, 1993.
[13] J Weickert, “Coherence enhancing diffusion,” *International Journal of Computer Vision*, vol. 31, pp. 111–127, 1999.
[14] P G Batchelor, M Moakher, Atkinsonm D, F Calamante, and A Connelly, “A rigorous framework for diffusion tensor calculus,” *Magn. Reson. Med.*, vol. 53, pp. 221–225, 2005.
[15] J Qi and R M Leahy, “Iterative reconstruction techniques in emission computed tomography,” *Phys Med. Biol.*, vol. 51, pp. R541–R578, 2006.
[16] K Vunckx, A Atre, K Baete, A Reilhac, CM Deroose, K Van Laere, and J Nuyts, “Evaluation of three MRI-based anatomical priors for quantitative PET brain imaging,” *IEEE Trans. Med. Imag.*, vol. 31(3), pp. 599–612, 2012.